JOURNAL OF MATERIALS SCIENCE 21 (1986) 389–394

On the formation of the stircast structure

J. M. M. MOLENAAR, L. KATGERMAN, W. H. KOOL
Laboratory of Metallurgy, Delft University of Technology, Rotterdamseweg 137, 2628 AL Delft, The Netherlands

R. J. SMEULDERS
Department of Applied Physics, Delft University of Technology, Lorentzweg 1, 2628 CJ Delft, The Netherlands

The conditions of solidification in a stirred bulk liquid are investigated to explain the non-dendritic microstructure of stircast alloys. A model of stirred solidification is presented, which allows a comparison of the solidification behaviour of metal alloys and organic analogues. This shows that nucleation and growth of solid in a bulk liquid is facilitated under the influence of stirring, provided the Prandtl-number is greater than unity. It is shown further that the solute gradient ahead of the solid–liquid interface of floating particles in a bulk liquid is reduced by the fluid flow. Combined with the thermal properties, and in analogy with the constitutional supercooling criterion, it is shown that solid growth in metals is likely to be cellular in an early stage of the solidification. In contrast, in stirred organic analogues, the solidification is dendritic in the early stage.

1. Introduction

In a previous paper [1], it was shown that cell-spacings of the coarse primary phase in stircast Al–6Cu (Al–6 wt % Cu, sometimes referred to as AlCu6) are considerably greater than secondary dendrite arm spacings in unstirred solidified Al–6Cu at equal solidification times. It was suggested that the convection causes the ratio of the thermal gradient in the liquid at the interface of floating primary crystals and the growth rate to be so small that the morphological type of growth becomes cellular. The purpose of this paper is to discuss the conditions in stirred solidification, and the validity of this suggestion. Results from the previous work [1] are related to results of similar batch-type stircasting experiments, performed with the organic substance neopentylalcohol in water, which have been published elsewhere [2, 3].

2. Experimental observations

In this section, the morphological similarities and differences in the microstructures of stircast Al–6Cu alloy and an organic analogue, neopentylalcohol (NPA) are summarized.

Fig. 1 shows a typical example of a slowly solidified stircast duplex-structure, of Al–6Cu [1]. The microstructure is typically non-dendritic. The primary particles consist of agglomerated cells. Fig. 2 shows the structures of quickly solidified, stirred and unstirred samples, respectively. The microstructure in Fig. 2a is also non-dendritic, whereas in Fig. 2b the normal dendritic structure is shown. Compared to the structure in Fig. 1, that in Fig. 2a is finer, as a result of a higher cooling rate [1]. At greater magnification, so-called rosette-type particles are often observed in quickly solidified stircast structures, see Fig. 3a. Such particles have been observed in earlier investigations [4–7]. It was suggested that they survive from being fragmented, when either stirring times are short, or agitation is not too intense [4, 5]. At long stirring times, the rosettes are replaced by particles consisting of radially grown cells, e.g. as in Fig. 3b. The solidification interface in these particles shows resemblance with classical examples of the cellular interface [8].

Similar stirring experiments have been performed using NPA (1.5 wt % H_2O). For experimental details, the reader is referred to the original publications [2, 3]. This organic substance is assumed to be a suitable analogue for metal alloys. Its Jackson α-factor, defined by the ratio of the solid–liquid interfacial energy and the entropy of fusion, is approximately 1.4 [9]. This is slightly greater than that of succinodinitrile (SDN) (1.34, [10]), an organic substance which is often used as an analogue for metals. In these experiments, dendrite-fragmentation has been observed in the early stages of the solidification, as shown in Fig. 4a. At long stirring times, primary dendrites disappear and are replaced by non-dendritic particles composed of cells. These particles which are shown in Fig. 4b, resemble those observed in stircast structures of Al–6Cu and other alloys.

In short, it is seen in the above figures that the particle morphology in Al–6Cu and NPA is similar in slowly cooled stircast samples, i.e. with long stirring times. A difference in the solidification of Al–6Cu and NPA is observed in early stages of solidification: in NPA, the primary particles observed are equiaxed dendrites, whereas in Al–6Cu, the rosette-type particles have a cellular appearance.

In addition, an experimental result obtained with NH_4Cl/H_2O mixtures is quoted here: Sens [11] observed that the growth of solid at a chilled wall is suppressed, while nucleation and growth of solid in

0022–2461/86 $03.00 + .12

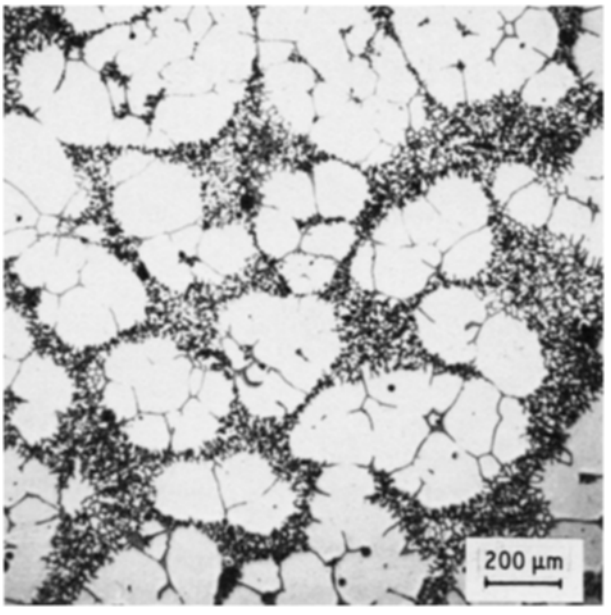

Figure 1 Typical duplex structure of stircast Al–6Cu, stirred for 400 sec, in the solid–liquid region, then quenched.

the bulk are enhanced, due to stirring in the bulk liquid. In the following, a theoretical interpretation of the experimental results in this section is given.

3. Stirred solidification model

The principal difference between stirred and unstirred (directional) solidification, with respect to the heat flow, is schematically shown in Fig. 5. In the conventional case, sketched in Fig. 5a, heat-flow is unidirectional from the liquid through the solid towards the chilled surface. The thermal gradient at the solid–liquid interface is positive. In contrast, during stircasting schematically represented in Fig. 5b, the latent heat evolved is taken from the solid particles through the liquid. To allow for this, the liquid has to be supercooled. The thermal gradient at the solid–liquid interface is negative.

In the following, it is shown that growth of solid from a chilled mould wall can be suppressed by stirring, if the Prandtl-number is greater than unity. Then, growth of solid in the bulk liquid is facilitated. Because the bulk liquid is supercooled, the growth of solid in the bulk is expected to be dendritic. This is not true when the Prandtl-number is much smaller than unity. Then the thermal gradient in the liquid at the solid–liquid interface is small. It is suggested that this leads to cellular growth of the solid during stircasting.

3.1. Inhibited growth at a chilled mould-wall

The boundary condition governing solid growth is given by

$$k_S G_S - k_L G_L = \varrho_S H R \qquad (1)$$

where k is the thermal conductivity (subscripts S and L refer to solid and liquid, respectively), G is the thermal gradient at the solid–liquid interface, ϱ the density, H the heat of fusion, and R the growth rate.

When the Prandtl-number is greater than unity, strong convection along a solid–liquid interface will reduce the thermal and mass-diffusion boundary layer thicknesses, and will increase the corresponding gradients at the interface. Considering the heat balance at the interface, Equation 1, the increased thermal gradient at the interface will result in a reduced growth rate R of the solid. This is explained below. In Fig. 6a, it is assumed that the growth of solid has started at a chilled wall, in the absence of convection. The dendrite-tip is growing at a tip undercooling ΔT_t. When stirring commences, the thermal and diffusion boundary layer thicknesses are reduced, and the corresponding thermal and concentration gradients increase, as illustrated in Fig. 6b. In Equation 1, $k_S G_S - k_L G_L$ may become negative, and the growth of solid at the chilled wall will stop. The gradient G_L will now conduct the superheat only. Until G_L is reduced to the critical gradient G_c, determined by the condition $k_S G_S - k_L G_c = 0$, the growth of solid remains inhibited. Provided the convection is sufficiently strong, the bulk-liquid becomes supercooled while the actual gradient G_L is greater than G_c, see

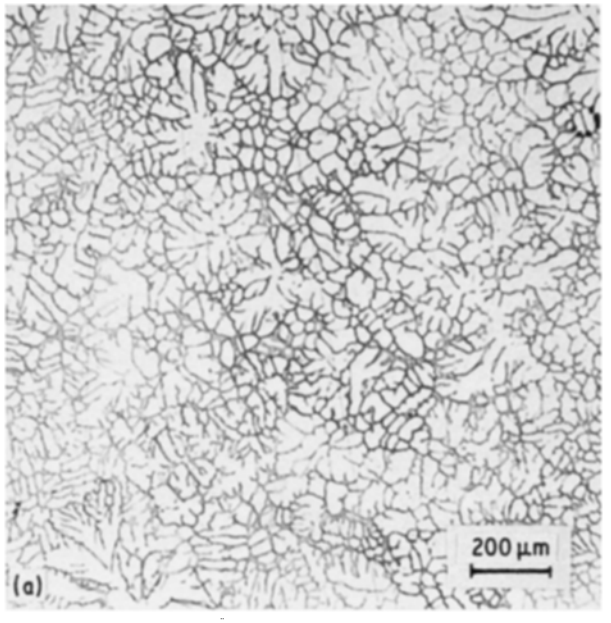

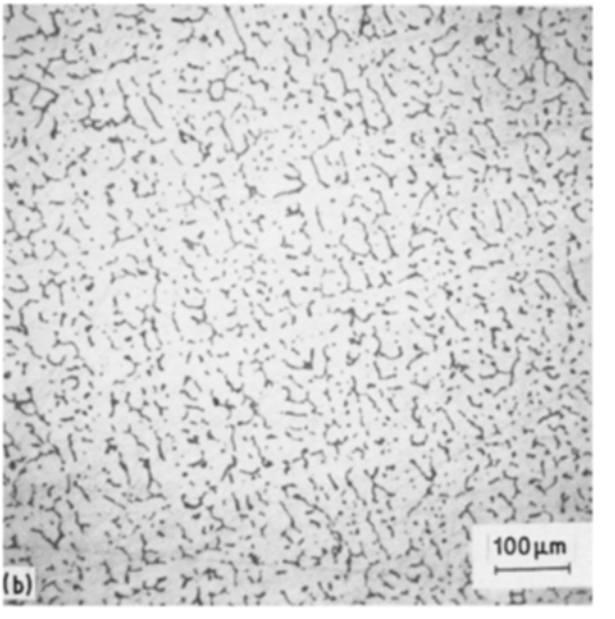

Figure 2 (a) Stircast structure of Al–6Cu stirred 8 sec in the solidus–liquidus region, then quenched. (b) Unstirred structure of Al–6Cu, obtained under the same conditions as (a), except stirring.

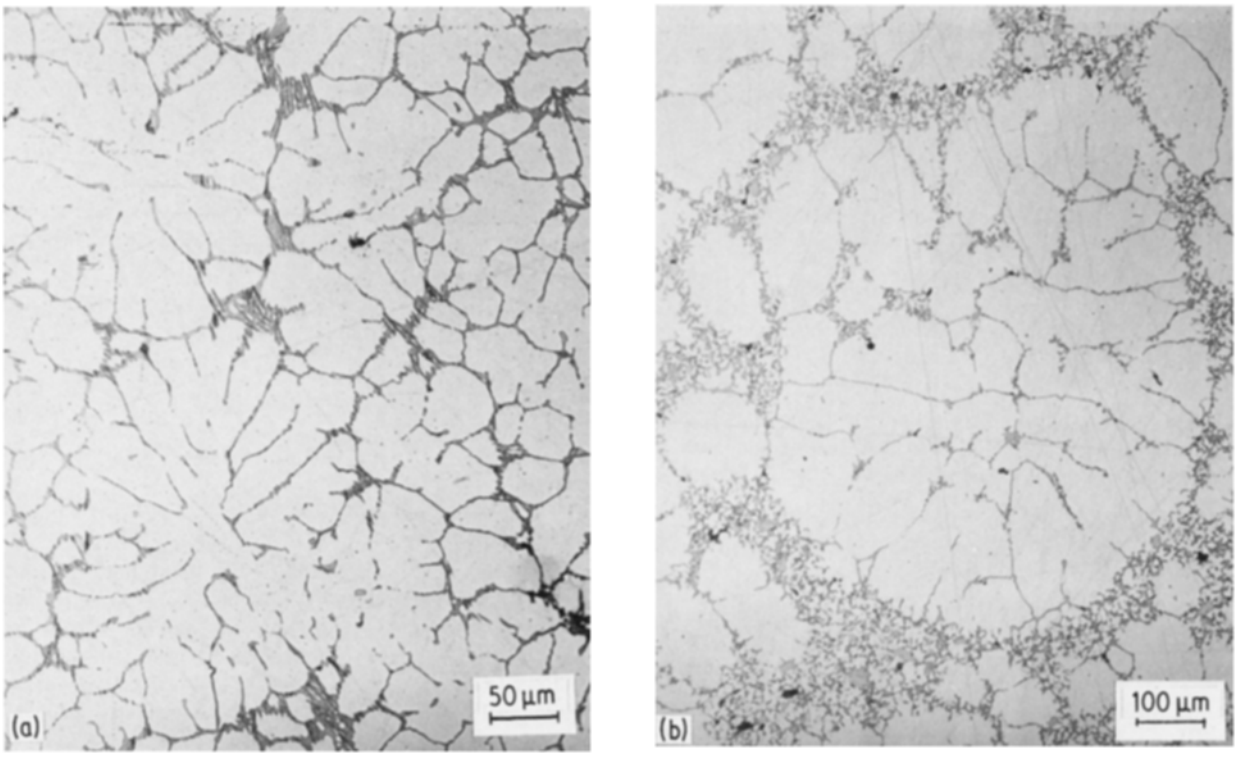

Figure 3 (a) Examples of rosette-type primary particles. The sample was stirred for 8 sec in the solidus–liquidus region, then quenched. (b) Primary particles in stircast AlCu6, consisting of radially grown cells; sample stirred for 540 sec in the solidus–liquidus region, then quenched.

Fig. 6c. When the Prandtl-number is greater than unity, e.g. with NH_4Cl/H_2O mixtures, this model explains that the growth of solid in the bulk-liquid is facilitated by stirring. This is confirmed by recent experimental observations [11].

For metal alloys, the Prandtl-number is small: ~ 0.01. This means that the thermal boundary layer thickness is much greater than the hydrodynamic boundary layer thickness. In this case the thermal gradient at the interface G_L will hardly be affected by stirring. For metal alloys, it is therefore unlikely that the growth of solid at the chilled mould-wall can be suppressed by stirring. More likely, the crystals in the bulk liquid grow from fragmented parts of the solid which grows at the chilled mould-wall. This has also been observed experimentally in simple stirring experiments performed in a crucible.

3.2. Fluid flow around floating particles in a bulk liquid

The fluid flow around floating particles in a field of constant shear can be written as a superposition of the externally applied field $\boldsymbol{v}^0$ and an additional flow $\boldsymbol{v}^1$, so that the condition of continuity is fulfilled at the particle surface and anywhere in the liquid volume:

$$\nabla \cdot \boldsymbol{v} = \nabla \cdot (\boldsymbol{v}^0 + \boldsymbol{v}^1) = 0 \qquad (2)$$

The following solution has been found for the special case of a sphere in a field of constant shear [12, 13]:

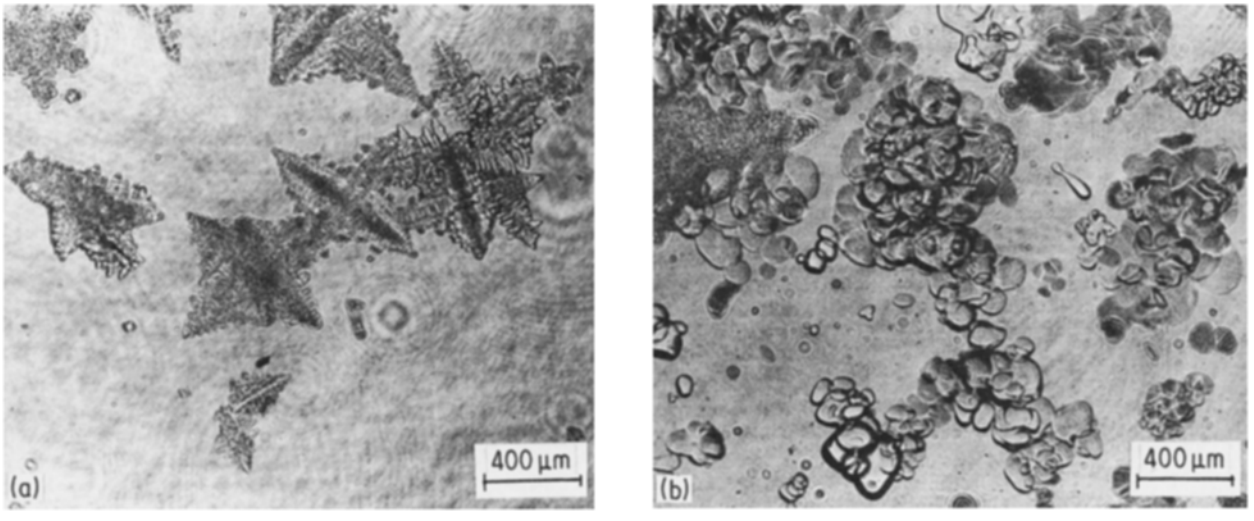

Figure 4 (a) Dendrite-fragmentation observed in stirred solidification of neopentylalcohol. (b) Morphological transition in stirred solidification of neopentylalcolhol. Primary particles consisting of cells resemble those in slowly cooled Al–6Cu stircast structures, compare with Fig. 1.

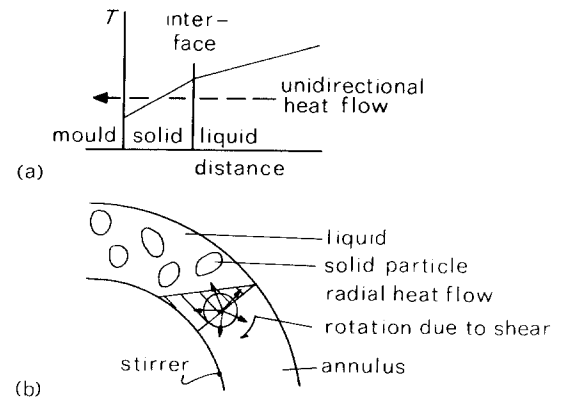

Figure 5 Different heat flow conditions in conventional chill-casting and stircasting. (a) Unidirectional heat flow in conventional chill-casting; (b) radial heat flow in stircasting.

$$v_i^1 = -\frac{5}{2}\frac{R^3}{r^5}\left(1-\frac{R^2}{r^2}\right)a_{jk}^0 x_i x_j x_k - \frac{R^5}{r^5}a_{ik}^0 x_k \qquad (3)$$

where $r^2 = x_1^2 + x_2^2 + x_3^2$ and in which R is the radius of the sphere, $a_{ij}^0 = \partial v_i/\partial x_j$ are the velocities of deformation, and x_1, x_2, x_3 the co-ordinates of a location in the flow field. In a rectangular co-ordinate system, the components are (in Vand's original paper [12], an error was introduced):

$$\begin{aligned} v_x^1 &= -\dot\gamma\left[\frac{5}{2}\frac{R^3x^2y}{r^5}\left(1-\frac{R^2}{r^2}\right)+\frac{1}{2}\frac{R^5y}{r^5}\right] \\ v_y^1 &= -\dot\gamma\left[\frac{5}{2}\frac{R^3xy^2}{r^5}\left(1-\frac{R^2}{r^2}\right)+\frac{1}{2}\frac{R^5x}{r^5}\right] \\ v_z^1 &= -\dot\gamma\left[\frac{5}{2}\frac{R^3xyz}{r^5}\left(1-\frac{R^2}{r^5}\right)\right] \end{aligned} \qquad (4)$$

where $\dot\gamma$ is the shear rate. The following formula can be used to find the components in a spherical co-ordinate system:

$$\begin{bmatrix} v_r^1 \\ v_\phi^1 \\ v_\theta^1 \end{bmatrix} = \begin{bmatrix} \cos\phi\sin\theta & \sin\phi\sin\theta & \cos\theta \\ -\sin\phi & \cos\phi & 0 \\ \cos\phi\cos\theta & \sin\phi\cos\theta & -\sin\theta \end{bmatrix}\begin{bmatrix} v_x^1 \\ v_y^1 \\ v_z^1 \end{bmatrix} \qquad (5)$$

For a Searle flow (see Fig. 7), which can be represented as

$$v_x^0 = \dot\gamma y,\ v_y^0 = v_z^0 = 0 \qquad (6)$$

the sumfield, as seen by an observer, at the origin of the sphere, rotating with the same speed as the sphere, is given by

$$\begin{aligned} v_r^* &= \dot\gamma\frac{r}{2}\sin(2\phi)\sin^2\theta\left[1-\frac{5}{2}\frac{R^3}{r^3}+\frac{3}{2}\frac{R^5}{r^5}\right] \\ v_\phi^* &= \dot\gamma\frac{r}{2}\cos(2\phi)\sin\theta\left[1-\frac{R^5}{r^5}\right] \\ v_\theta^* &= \dot\gamma\frac{r}{4}\sin(2\phi)\sin(2\theta)\left[1-\frac{R^5}{r^5}\right] \end{aligned} \qquad (7)$$

The components of this field are zero at the surface of the sphere. Note, that the direction of the flow changes as a function of ϕ and θ, the consequences of which will be further investigated in the next section.

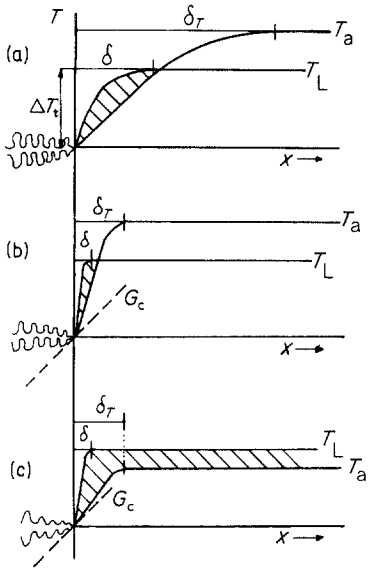

Figure 6 Illustration of the suppressed growth of solid at a chilled wall, for Pr $\geqslant$ 1. T_a represents the actual temperature distribution, T_L the equilbrium liquidus temperature distribution, x is the distance from the solid–liquid interface. The diffusion boundary layer is indicated by δ, the thermal boundary layer thickness by δ_T. (a) Conventional case, no stirring. The dendrite is growing at tip undercooling ΔT_t, in a constitutionally supercooled liquid (shaded area). (b) Suppressed growth at the interface by stirring. Thermal and diffusion boundary layer δ_T and δ, respectively, are reduced by convection, and the corresponding thermal and solute gradient at the interface have increased. G_c is the critical temperature gradient defined in the text. (c) Condition at the interface, some time after the condition sketched in Fig. 6b. The actual gradient at the interface is still greater than G_c, so that growth is suppressed, while the bulk liquid has become supercooled. This facilitates nucleation and growth in the bulk liquid.

3.3. Regimes of diffusion and convection

Assuming that the radial component of the flow field, expressed by Equation 7 contributes to the heat and mass-transport at the interface, one can determine the distance from the surface of the sphere where the convection predominates the diffusion. The criterion for this is that the Peclet-number for the radial flow, which is defined by

$$\mathrm{Pe} = \frac{v_r^* L}{a} \qquad (8)$$

must be greater than 1. In Equation 8, L is a characteristic length (the diameter of the sphere), and a is either the thermal diffusivity, or the diffusion coefficient, depending on whether the temperature field or the concentration field is considered. Substituting $\varrho = r/R$

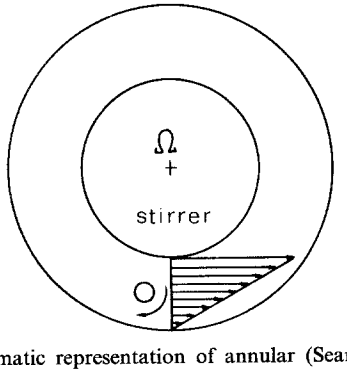

Figure 7 Schematic representation of annular (Searle type) fluid flow. Suspended particles rotate under the influence of a constant shear rate.

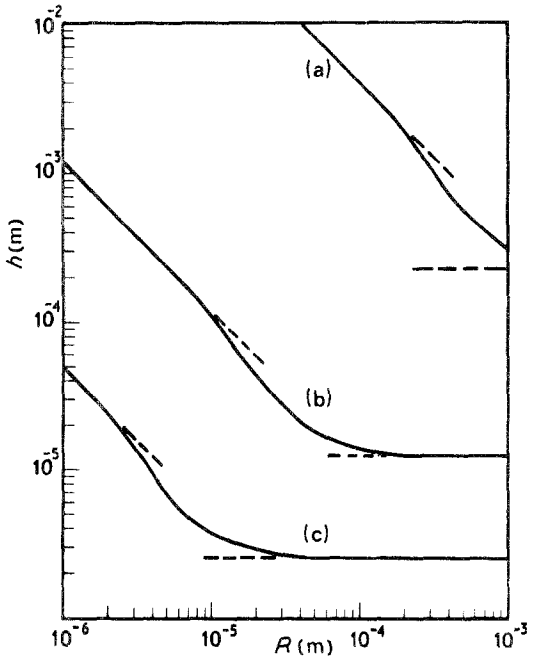

Figure 8 Graph of $h(R)$, representing the distance where the Peclet-number equals 1, for three cases in all of which $\dot{\gamma} = 100\,\text{sec}^{-1}$: (a) Al–Cu alloy, thermal diffusion, $a = 4 \times 10^{-5}\,\text{m}^2\,\text{sec}^{-1}$, (b) succinodinitrile, thermal diffusion, $a = 1.16 \times 10^{-7}\,\text{m}^2\,\text{sec}^{-1}$, (c) Al–Cu alloy and succinodinitrile, mass diffusion, $a \sim 5 \times 10^{-9}\,\text{m}^2\,\text{sec}^{-1}$. The function $h(R)$ defines regimes of predominant heat and mass transport, by convection and diffusion: above the curves transport by convection predominates (Pe > 1): below the curves transport by diffusion predominates (Pe < 1).

and solving Equation 8 for Pe = 1, leads to (for angles $\phi = 45°$, and $\theta = 90°$):

$$\varrho - \frac{5}{2\varrho^2} + \frac{3}{2\varrho^4} = \frac{a}{\dot{\gamma}R^2} \tag{9}$$

Evaluating $h = r - R$, it is easily found that provided $R \ll (a/\dot{\gamma})^{1/2}$, h approaches the value

$$h^{\infty} = \left(\frac{2}{15}\frac{a}{\dot{\gamma}}\right)^{1/2} \tag{10}$$

At small R, i.e. when $R \ll (a/\dot{\gamma})^{1/2}$, it follows from Equation 9 that $h = a/\dot{\gamma}R$. The function $h(R)$ is shown in Fig. 8 for $\dot{\gamma} = 100\,\text{sec}^{-1}$, and the three a-values corresponding to (i) heat transport in Al–6Cu ($a = 4 \times 10^{-5}\,\text{m}^2\,\text{sec}^{-1}$), (ii) heat transport in SDN ($a = 1.16 \times 10^{-7}\,\text{m}^2\,\text{sec}^{-1}$), and (iii) mass-transfer in Al–6Cu and SDN (based on data given by Wilcox [14] and Fisher [15], it is assumed that the diffusion coefficients are of the same order of magnitude, $a \sim 5 \times 10^{-9}\,\text{m}^2\,\text{sec}^{-1}$). It defines under which conditions the heat or mass-transport is dominated by diffusion or by convection. Note, that with decreasing particle radius, the distance over which transport by diffusion predominates, increases. This is because for small particles, the influence of the additional flow field, $\boldsymbol{v}^1$ in Equation 2, is small.

3.4. Stabilized growth of solid in a stirred bulk liquid

The crystals which grow in the bulk liquid have a temperature slightly in excess of that of the surrounding liquid. This enables the crystal to dispose of the latent heat relased at the interface, which means that the crystal can grow. For metals, the Prandtl-number is small, which expresses that the thermal boundary layer thickness is much greater than the hydrodynamic boundary layer thickness. As a consequence, the thermal gradient at the interface will be small. This can also be seen in Fig. 8. For a particle with a radius of 100 μm, in the case of SDN, the heat transport is dominated by convection at distances $h > 14\,\mu$m, while for Al–6Cu under the same conditions, this is true if $h > 4000\,\mu$m. With the same bulk supercooling in both cases, the thermal gradient in the case of Al–6Cu must be much smaller. This difference between Al–6Cu and SDN is the consequence of a much greater thermal diffusivity, or equivalently a much smaller Prandtl-number.

As the crystals grow and become more numerous, the temperature differences across the thermal boundary layers will decrease further, due to interaction of the thermal diffusion fields of the individual particles [16–18].

Again for a particle with a radius of 100 μm, Fig. 8 shows that the mass-transport by convection predominates that by diffusion at distances greater than 2 μm. Provided the diffusion boundary layer thickness is not much smaller than 2 μm, it can be concluded, that the solute peak at the solid–liquid interface of a floating particle is reduced due to the fluid flow around the particle. As a consequence, the equilibrium temperature distribution ahead of the interface will be almost uniform. Combined with the small negative thermal gradient at the interface, it follows that the amount of constitutional supercooling ahead of the interface is small.

Now, we have the analogy illustrated in Fig. 9, between stirred solidification and unidirectional solidification. For the latter case demonstrated in Fig. 9b, it has been shown theoretically and experimentally [19–24], that the growth morphology changes from the dendritic to the cellular type, before stability of the interface is achieved. Applied to stirred solidification in a bulk liquid, see Fig. 9a, the interface is stable when $G_L = 0$, a condition that cannot be achieved completely, so long as the growth rate R of the primary particles is positive. Based on this analogy, it is

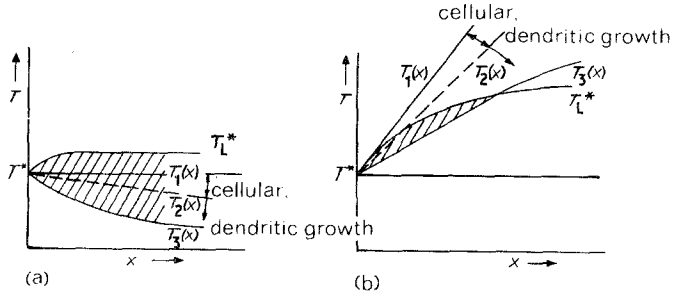

Figure 9 Constitutional supercooling at solid–liquid interface, (a) of a floating particle in a bulk liquid, and (b) in conventional solidification. Different temperature distributions $T_1(x)$, $T_2(x)$ and $T_3(x)$ are indicated: with $T(x) = T_1(x)$, the growth of solid is morphologically stable, with $T(x) > T_2(x)$, growth is cellular, with $T(x) < T_2(x)$ growth is dendritic.

suggested that the growth of solid in a stirred bulk liquid will be cellular, when G_L has become sufficiently small.

In organic substances, the thermal gradient at the interface of floating particles will be much greater than in metals. Based on the theory of interface stability [25], this indicates that, compared with metals, the interface of primary particles in the organic substances is considerably more unstable in the early stage of the solidification, as indeed has been confirmed by the observation of equiaxed dendrites, see Fig. 4a. In a later stage of the solidification, the thermal gradient will decrease, due to interaction of the thermal fields of the individual particles, and eventually the growth morphology will change to the cellular type. It is expected therefore, that the difference in the growth morphology of metals and organic analogues which occurs in the early stage of the stirred solidification will vanish at long stirring times. This is in agreement with the experimental results presented in Section 2.

4. Discussion

In the previous sections an attempt has been made to explain the differences in the stirred solidification of Al–6Cu and NPA. It has been made plausible that in the AlCu alloy, in the early stage of the solidification the morphological type of growth in the bulk liquid is cellular, while in NPA it is dendritic. Vogel and Cantor [26] have shown that stirring destabilizes the solid–liquid interface of particles growing in a bulk liquid. Based on this result, one would expect the growth of the primary phase in stirred solidification to be dendritic. To explain the typically non-dendritic character of stircast structures, a dendrite fragmentation mechanism was suggested by Vogel *et al.* [4, 18, 27]. However, because detached side branches are expected to continue to grow dendritically in the supercooled bulk liquid, this fragmentation mechanism cannot explain the increased cell-spacings observed in stircast microstructures [1], without an additional stabilizing influence. Following Jackson *et al.* [16], Doherty *et al.* [18] have suggested that this stabilizing influence arises from the interaction of the thermal diffusion fields of individual particles. The present paper attempts to show in fact, that the reduced solute gradient and the small thermal gradient at the interface are sufficient for the growth to be cellular from the start of the solidification. The increased cell-spacings observed in stircast structures [1] are in agreement with this morphological type of growth.

5. Conclusions

1. Rosette-type particles often observed in microstructures of stircast metal alloys can be explained as the result of cellular growth.

2. At short distances ahead of the solid–liquid interface of floating primary particles in a stirred bulk liquid, mass-transport by convection predominates that by conduction.

3. The fluid flow around floating particles in a stirred bulk liquid is insufficient for the heat transport to be predominated by convection.

4. The difference in the solidification behaviour of Al–6Cu and neopentylalcohol in the early stage of the stirred solidification can be ascribed to the different thermal properties (Prandtl-number) of these substances.

References

1. J. M. M. MOLENAAR, F. W. H. C. SALEMANS and L. KATGERMAN, *J. Mater. Sci.* **20** (1985) 4335.
2. R. J. SMEULDERS, F. H. MISCHGOFSKY and H. J. FRANKENA, Proceedings of the International Conference on Optical Techniques in Process Control, The Hague, The Netherlands, June 1983, edited by H. S. Stephens and C. A. Stapleton (British Hydromechanics Research Association, Cranfield, 1983) p. 265.
3. R. J. SMEULDERS, PhD thesis, Delft University of Technology, The Netherlands, (1984).
4. A. VOGEL, R. D. DOHERTY and B. CANTOR, Proceedings of the International Conference on Solidification and Casting of Metals, University of Sheffield, July 1977 (The Metals Society, London, 1979) p. 518.
5. M. A. TAHA and N. A. EL-MAHALLAWY, 46th International Foundary Congress, Madrid, 1979, (Asociation Tecnica y de Investigacion de Fundicion, Madrid, 1979) paper no. 15.
6. N. APAYDIN, K. V. PRABHAKAR and R. D. DOHERTY, *Mater. Sci. Eng.* **46** (1980) 145.
7. J. C. VAN DAM and F. H. MISCHGOSFSKY, *J. Mater. Sci.* **17** (1982) 989.
8. R. M. SHARP and A. HELLAWELL, *J. Cryst. Growth* **11** (1971) 77.
9. J. C. VAN DAM, private communication.
10. M. E. GLICKSMAN, R. J. SCHAEFFER and J. D. AYERS, *Metall. Trans.* **7A** (1976) 1747.
11. H. SENS, Ir thesis, Delft University of Technology. The Netherlands (1983).
12. V. VAND, *J. Phys. Colloid Chem.* **52** (1948) 277.
13. L. LANDAU and E. M. LIFSHITZ, "Fluid Mechanics", 5th Edn (Pergamon, 1978) p. 77.
14. W. R. WILCOX, in "Preparation and properties of Solid State Materials", Vol. 1, edited by R. A. Lefever (Marcel Dekker, New York, 1971) Ch. 2.
15. D. J. FISHER, PhD thesis (301), Ecole Polytechnique Federale de Lausanne, Switzerland (1978).
16. K. A. JACKSON, J. D. HUNT, D. R. UHLMANN and T. P. SEWARD III *Trans. AIME* **236** (1966) 149.
17. M. H. BURDEN and J. D. HUNT, *Metall. Trans.* **6A** (1975) 240.
18. R. D. DOHERTY, H. I. LEE and E. A. FEEST, *Mater. Sci. Eng.* **65** (1984) 181.
19. D. WALTON, W. A. TILLER, J. W. RUTTER and W. C. WINEGARD, *Trans. AIME* **203** (1955) 1023.
20. T. S. PLASKETT and W. C. WINEGARD, *Can. J. Phys.* **37** (1959) 1555.
21. W. BARDSLEY, J. M. CALLAN, H. A. CHEDZEY and D. T. J. HURLE, *Solid State Electron.* **3** (1961) 142.
22. G. S. COLE and W. C. WINEGARD, *J. Inst. Met.* **92** (1963) 322.
23. H. D. HUNT, J. A. SPITTLE and R. W. SMITH, "The Solidification of Metals", ISI Publ. no. 110 (Iron and Steel Institute, London, 1967) p. 57.
24. J. O. COULTHARD and R. ELLIOTT, *ibid.* p. 61.
25. W. W. MULLINS and R. F. SEKERKA, *J. Appl. Phys.* **35** (1964) 444.
26. A. VOGEL and B. CANTOR, *J. Cryst. Growth* **37** (1977) 309.
27. H. I. LEE, R. D. DOHERTY, E. A. FEEST and J. M. TITCHMARSH, Proceedings of the International Conference on Solidification Technology in the Foundry and Casthouse, Warwick, Coventry, 1980 (The Metals Society, London, 1983) p. 119.

Received 3 May
and accepted 18 December 1984